

# Solitons in Tonks-Girardeau gas with dipolar interactions

B B Baizakov<sup>1</sup>, F Kh Abdullaev<sup>1</sup>, B A Malomed<sup>2</sup> and M Salerno<sup>3</sup>

<sup>1</sup> Physical - Technical Institute, Uzbek Academy of Sciences, 2-b, G. Mavlyanov str., 100084, Tashkent, Uzbekistan

<sup>2</sup> Department of Physical Electronics, School of Electrical Engineering, Faculty of Engineering, Tel Aviv University, Tel Aviv 69978, Israel

<sup>3</sup> Dipartimento di Fisica “E. R. Caianiello”, Consorzio Nazionale Interuniversitario per le Scienze Fisiche della Materia (CNISM), Università di Salerno, I-84081, Baronissi (SA), Italy

E-mail: baizakov@uzsci.net, fatkh@uzsci.net, malomed@eng.tau.ac.il, salerno@sa.infn.it

**Abstract.** The existence of bright solitons in the model of the Tonks-Girardeau (TG) gas with dipole-dipole (DD) interactions is reported. The governing equation is taken as the quintic nonlinear Schrödinger equation (NLSE) with the nonlocal cubic term accounting for the DD attraction. In different regions of the parameter space (the dipole moment and atom number), matter-wave solitons feature flat-top or compacton-like shapes. For the flat-top states, the NLSE with the local cubic-quintic (CQ) nonlinearity is shown to be a good approximation. Specific dynamical effects are studied assuming that the strength of the DD interactions is ramped up or drops to zero. Generation of dark-soliton pairs in the gas shrinking under the action of the intensifying DD attraction is observed. Dark solitons exhibit the particle-like collision behavior. Peculiarities of dipole solitons in the TG gas are highlighted by comparison with the NLSE including the local CQ terms. Collisions between the solitons are studied too. In many cases, the collisions result in merger of the solitons into a breather, due to strong attraction between them.

PACS numbers: 42.65.Tg, 42.65.Sf

Submitted to: *J. Phys. B: At. Mol. Phys.*

## 1. Introduction

The experimental realization of degenerate Bose gases in tight effectively one-dimensional (1D) traps [1] in the Tonks-Girardeau (TG) regime [2] has rekindled interest to the TG model, which, being well known for a long time, was assumed to have a theoretical value only (for a review see [3]). In the TG state, bosons emulate the Pauli exclusion principle, as a result of the hard-core repulsion, rather than as a manifestation of the quantum statistics. One of recent trends in this field is the application of mean-field-like approaches to the description of macroscopic dynamics of TG gases [4, 5]. The starting point of this approach is the use of a formal analogy between hydrodynamic equations for degenerate Fermi gases and Bose gases in the TG phase. This analogy has led to the derivation of the nonlinear Schrödinger equation (NLSE) with the local quintic repulsive nonlinearity for the “wave function” of the TG gas [4]. In the framework of the quintic NLSE, the existence of dark solitons was predicted [4, 6], and dynamics of dark solitons was investigated [7]. Bright solitons of the gap type in the same model equation including a periodic optical-lattice (OL) potential have been reported too, although in different contexts, such as a phenomenological description of degenerate Fermi gases and BCS superfluids, [8]-[10]. The quasi-mean-field approach relies on the physically plausible assumption that the spatial scale of variations of the gas density is much larger than the healing length. Under this condition, the effective NLSE allows one to approximate collective oscillations of the TG gas in a harmonic trap. Indeed, it has been demonstrated that excitation frequencies derived from the fermionic hydrodynamic equations, and from the quintic NLSE agree within a few percent [11, 12].

A natural extension of this line of research is to consider gases with long-range dipole-dipolar (DD) interactions between atoms. Some bosonic atoms, such as  $^{52}\text{Cr}$ , feature a significant permanent magnetic dipole moment ( $\simeq 6\mu_B$ , in the case of chromium). The creation of the Bose-Einstein condensate (BEC) made of  $^{52}\text{Cr}$ , and various experiments in that quantum gas have been reported [13, 14, 15]. A gas of LiCs molecules carrying a permanent electric dipole moment was also recently made available to experiments [16]. In addition to that, atoms may be polarized by an external dc electric field [17].

The nonlocal character of the DD interactions may drastically modify properties of the quantum gas – first of all, changing the character of the collapse in it [14]. Further, stable isotropic [18] and anisotropic [19] 2D solitons have been predicted in the 2D dipolar BEC, whereas such localized states are always unstable in the same model with local interactions [20]. Recently, families of 1D matter-wave solitons in a Bose-Einstein condensate supported by the competition of contact and dipole-dipole interactions of opposite signs were predicted in Ref. [21], and 1D discrete solitons corresponding to the limit case of the dipolar condensate trapped in a very deep OL (i.e., solutions to the discrete NLSE with the long-range DD interactions between lattice sites) were found too [22]. It is relevant to mention that qualitatively similar effects may be induced by the nonlocal nonlinearity in models of optical media [23, 24].

In this work, we study localized structures in the model of a 1D Bose gases supported by competing nonlocal attractive cubic (DD) and local repulsive quintic (contact) nonlinearities, using numerical simulations of the NLSE containing this combination of the nonlinear terms. Besides the cold bosons in the TG regime, this model may apply (at least, at the phenomenological level [9]) to nearly-1D degenerate Fermi gases with DD interactions between atoms.

The paper is structured as follows. In Section II we introduce the model, present typical shapes of solitons expected in the TG dipolar gas, and study their stability in direct simulations. In Section III we demonstrate, via numerical experiments, dynamics predicted by the model with a *variable* (time-dependent) strength of the DD interactions, including formation of dark solitons on top of a broad bright soliton, splitting of the soliton, and expansion of the TG gas, in cases when the DD interaction is ramped up, or switched off. In Section IV, we report various results of interactions and collisions between two solitons. Section V concludes the paper.

## 2. The model and numerical analysis

In accordance with what was said above, we start with the quintic NLSE introduced in Ref. [4], to which we add the nonlocal cubic term accounting for the DD interaction:

$$i\psi_t + \frac{1}{2}\psi_{xx} - \pi^2 N^2 |\psi|^4 \psi + 2Nd^2 \psi(x, t) \int_{-\infty}^{+\infty} R(|x-x'|) |\psi(x', t)|^2 dx' = 0, \quad (1)$$

where  $N$  is the total number of atoms, and  $d$  is the atomic dipole moment, the wave function being subject to the normalization condition,

$$\int_{-\infty}^{+\infty} |\psi(x)|^2 dx = 1. \quad (2)$$

Equation (1) is expected to be valid for large number of atoms  $N$ , typically  $\gg 10$ , when oscillations of the matter-wave density along the chain of strongly interacting bosons confined to a tight waveguide are essentially suppressed. On the other hand, the Bose-Fermi mapping, which underlies the solution of the TG model [2], may hold in the present situation provided that the dipolar attraction between atoms is weaker than the contact (hard-core) repulsion. These conditions may be together expressed as  $N \gg 2d^2/(\pi^2\xi)$ , where  $\xi$  is the healing length, which is of order one in the present notation. We assume that the dipoles are oriented along the  $x$  axes, hence and the configuration possesses the cylindrical symmetry.

The model based on Eq. (1) has been studied in detail in some limit cases. With  $R(x) = \delta(x)$ , the equation reduces to the ordinary cubic-quintic (CQ) NLSE, which supports a fully stable family of bright-soliton solutions in a finite range of the chemical potential [25]. On the other hand, if the quintic term is absent, Eq. (1) reduces to the NLSE with nonlocal cubic nonlinearity, whose solutions were studied too, see, e.g., Refs. [26]. The degree of non-locality is quantified by the ratio between the soliton's width and spatial extent of nonlocal response function  $R(x)$ . Depending on this ratio, qualitatively different behaviors can be observed. Namely, in the case of strong nonlocality, i.e.,

when the characteristic nonlocal response length is greater than the soliton's width, a sinusoidally “breathing” mode (the so-called “accessible soliton”) was predicted [27] and experimentally observed [28]. In the opposite situation, when the width of the response function is small compared to the soliton's size, the governing equation may be approximated by a modified NLSE [29].

As the kernel in Eq. (1) we use

$$R(x) = \sqrt{\pi}(1 + 2x^2) \exp(x^2) \operatorname{erfc}(|x|) - 2|x|, \quad (3)$$

which was derived for the dipolar BEC in the quasi-1D trap [30], assuming that the dipole moments are fixed (by an external magnetic field) along axis  $x$ , hence the DD interaction is attractive.

As said above, Eq. (1) with the long-range attraction gives rise to stable solitons in the absence of the quintic repulsive term, a distinctive feature of these solitons being the breathing intrinsic mode that may be easily excited [27]. Effects produced by the quintic term in numerically found solutions increase with  $N$ , leading to broadening of the localized state, as shown in Fig. 1, which displays soliton solutions found by means of the imaginary-time relaxation method.

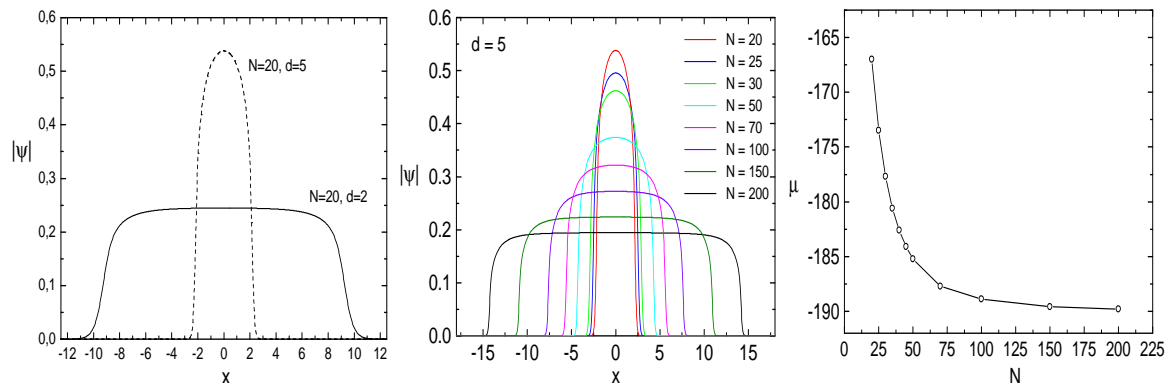


**Figure 1.** (Color online) Stationary localized states of Eq. (1), found by means of the numerical integration in imaginary time. Left panel: Effect of increasing strength of dipolar interactions at constant number of atoms ( $N = 20$ ). Soliton is broad (narrow) at weaker (stronger) dipolar interactions. Middle panel: Effect of increasing number of atoms at constant strength of dipolar interactions ( $d = 5$ ). Soliton broadens as the number of atoms increases. Right panel: Chemical potential as a function the number of atoms for configurations shown in the middle panel.

To check the stability of the localized stationary solutions to Eq. (1), we ran simulations in the real time, adding spatially random perturbations to the initial state. The solitons were observed to shed off the perturbations, in the form of linear waves, and quickly restored their stationary form, as demonstrated in Fig. 2, which clearly demonstrates that the localized states are stable. A first evidence of the stability of solitons can be seen on the right panel of Fig. 1, where the chemical potential is drawn as a function of the number of atoms. Negative slope of the curve ( $d\mu/dN < 0$ ) is the indication of stability of solitons according to the Vakitov - Kolokolov criterion [31].

At large number of atoms ( $N > 100$  for  $d = 5$ ), when the soliton acquires a "flat-top" shape, the slope becomes vanishing and the VK criterion does not apply in a strong sense (marginal VK stability). For "flat-top" solitons computation of the chemical potential using the exact solution (see below Eq. (5)), rather than solution found from the imaginary time propagation method, indeed gives the constant value  $\mu = -190$  for the whole interval of  $N$  shown on the right panel of Fig. 1.

Despite the indefinite character of the VK criterion in this case, the direct analysis demonstrates that, in the model with the competing nonlinearities considered in this work, which correspond to the attractive nonlocal cubic and repulsive local quintic terms, all bright solitons turn out to be stable. To check the stability of the localized stationary solutions to Eq. (1), we ran simulations in the real time, adding spatially random perturbations to the initial state. The solitons were observed to shed off the perturbations, in the form of linear waves, and quickly restored their stationary form, as demonstrated in Fig. 2, which clearly demonstrates that the localized states are stable.

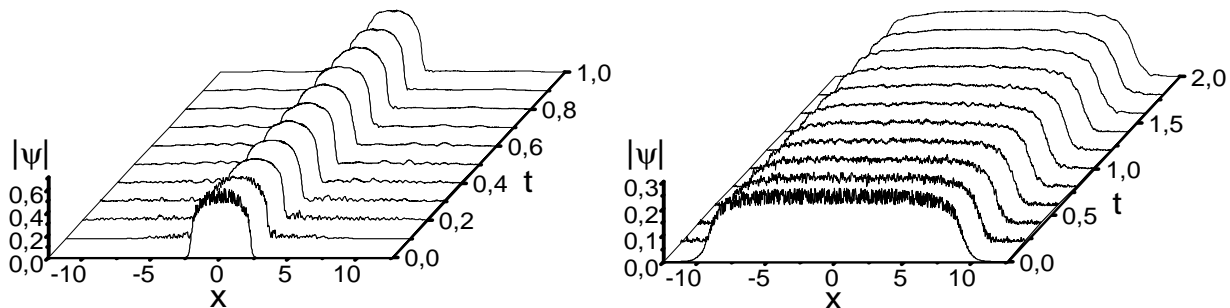


**Figure 2.** Left panel: The evolution of the soliton with  $N = 20$  and  $d = 5$ , depicted in Fig. 1 by the dashed line, which was initially perturbed by adding random noise,  $\psi(x, 0) = \psi_{\text{sol}}(x)[1 + \sigma(x)]$ , where  $\sigma(x)$  is a random function of  $x$ , uniformly distributed in interval  $[-0.25, +0.25]$  (note that this perturbation is not really small). Right panel: A similar verification of the stability of the flat-top dipole soliton with  $N = 20$  and  $d = 2$ , shown by the solid line in Fig. 1.

All numerical simulations were performed by dint of the split-step fast-Fourier-transform method [33] in a spatial domain of length  $L = 8\pi$  with 1024 modes. The time step was  $\delta t = 0.001$ . To control the accuracy of numerical results, we monitored the accuracy of normalization condition (2). During the entire simulation, it was held to the relative precision better than  $10^{-3}$ . To prevent re-entering of the linear waves emitted by the perturbed soliton into the integration domain, absorbers were installed at domain boundaries. Actually, this numerical procedure is a straightforward extension of that used for simulations of the NLSE in real time [34], and imaginary-time propagation method for finding ground states in NLSE-based models [35]. In the numerical results presented below we assumed that the ground state of the configuration is attained if the variation of the chemical potential

$$\mu = \int_{-\infty}^{\infty} \left( \frac{1}{2} |\psi_x|^2 + \pi^2 N^2 |\psi|^6 - 2d^2 N |\psi|^2 \int_{-\infty}^{+\infty} R(|x - x'|) |\psi(x', t)|^2 dx' \right) dx,$$

in the course of integration becomes less than  $d\mu \sim 10^{-8}$ .

Shapes of localized states in Fig. 1 are determined by the long-range DD forces and short-range contact repulsion for a particular number of atoms in the TG gas. Having analyzed a large body of numerical results, we can conclude that, for a moderate size of the dipole moment,  $d$ , the soliton develops a “flat-top” shape. In the case of the strong DD interaction, the soliton becomes a “compacton”, with very short tails. In fact, the latter case corresponds to the Thomas-Fermi limit, when the kinetic-energy term in Eq. (1) is negligible, while the integral term in Eq. (1) plays the role of an effective potential in which the locally repulsive TG gas is trapped. Then, stronger DD interactions mean a tighter trapping potential with steep walls induced by kernel function (3).

It is pertinent to mention that, in contrast to the recently considered model of dipolar BEC with competing cubic local and nonlocal interactions [21], in the present model, which is of the CQ type, parameter  $N$  cannot be eliminated from governing equation (1) by a rescaling of the wave function. This is the key point explaining the existence of arbitrarily broad flat-top solitons in the model. On the other hand, if a broad flat-top bright soliton is available, one may consider it as a background for dark solitons. The advantage of this setting is a possibility to explore dark solitons and their interactions on top of the uniform background, which is distinct from the usual situation when the quantum gas is confined by a harmonic trap, hence the background matter-wave density is nonuniform [32] (see below).

If the soliton’s width greatly exceeds that of kernel (3), which takes place at  $N \gg d^2$ , Eq. (1) is reduced to the local NLSE with the CQ nonlinearity. Considering the local counterpart of Eq. (1), we replace  $R(x) \rightarrow 2\delta(x)$ , because  $\int_{-\infty}^{\infty} R(x)dx = 2$ . Then the corresponding local NLSE acquires the form of

$$i\psi_t + \frac{1}{2}\psi_{xx} - \alpha|\psi|^4\psi + \beta|\psi|^2\psi = 0, \quad (4)$$

where notation  $\alpha = \pi^2 N^2$ ,  $\beta = 4d^2 N$  is introduced.

Exact soliton solutions to Eq. (4) were found in Ref. [25]. For the case of the self-focusing cubic ( $\beta > 0$ ) and defocusing quintic ( $\alpha > 0$ ) nonlinearities, the solution is (under normalization condition (2))

$$\psi(x, t) = \sqrt{\frac{3\beta}{4\alpha}} \frac{\tanh(\eta) \exp[i(qx - \mu t)]}{\sqrt{1 + \operatorname{sech}(\eta)\cosh(x/a)}}, \quad \eta \equiv \sqrt{\frac{2\alpha}{3}}, \quad a \equiv \frac{1}{\beta} \frac{\eta}{\tanh(\eta)}, \quad (5)$$

where  $q$  and  $\mu$  stand for the wave vector and chemical potential of the soliton. An example of stationary solution of Eq. (4) for a particular set of parameters, compared with the solution of original Eq. (1), is presented in Fig. 3.

As seen from this figure, the solutions of nonlocal equation (1) with kernel (3), and of the local NLSE are in a qualitative agreement. Therefore, exact solutions (5) of the local equation may be used as appropriate initial conditions for simulations of Eq. (1).

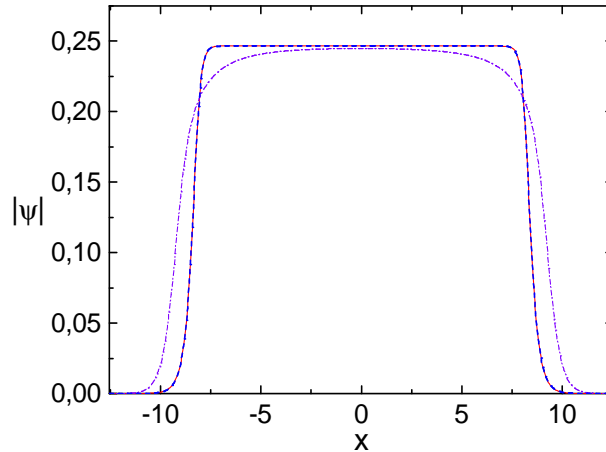


**Figure 3.** (Color online) Comparison of soliton profiles as generated by the imaginary-time relaxation method, applied to Eq. (1) (the dash-dotted purple line) and to the local equation with the cubic-quintic nonlinearity, Eq. (4) (the solid red line), and as predicted by exact solution (5) to the latter equation (the dashed blue line), for  $N = 20$ ,  $d = 2$ . The two latter profiles are indistinguishable, being juxtaposed to illustrate the accuracy of the numerical procedure.

### 3. Soliton dynamics under varying dipolar interaction

Properties of solitons can be studied under a varying strength of the DD interaction. In the experiments, it may be varied in time by changing the orientation of dipoles with respect to the axial direction, rotating the external magnetic field [15], or by changing the strength of the external electric field, if the atomic dipole moment is induced by the latter field [17].

Below we present numerical simulations of Eq. (1) with variable coefficient  $d(t)$ . With this objective in mind, we first prepare the ground-state solution of Eq. (1) by means of the imaginary-time propagation method, as explained in the previous section. Then we insert this solution into Eq. (1) as the initial condition, and simulate the evolution in real time, with  $d$  substituted by  $d(t)$  of a chosen form.

#### 3.1. Contraction of the TG gas by strengthening the dipolar interaction

The stationary solitons in the model of the dipolar TG gas are formed due to the balance between the contact repulsion and long-range attraction between atoms. When the strength of one of these forces is varied in time, solitons naturally shrink or expand. The most significant observation following from the numerical simulations is that, when the strength of the DD interaction is swiftly ramped up, dark soliton-antisoliton pairs are created, as shown in Fig. 4 (here, “solitons” and “antisolitons” are defined as patterns with opposite signs of the phase gradient across the density depression, see the left panel in Fig. 6).

The number of the generated dark soliton-antisoliton pairs depends on the speed at which the dipolar interaction is ramped up. Reaching the edge of the flat-top

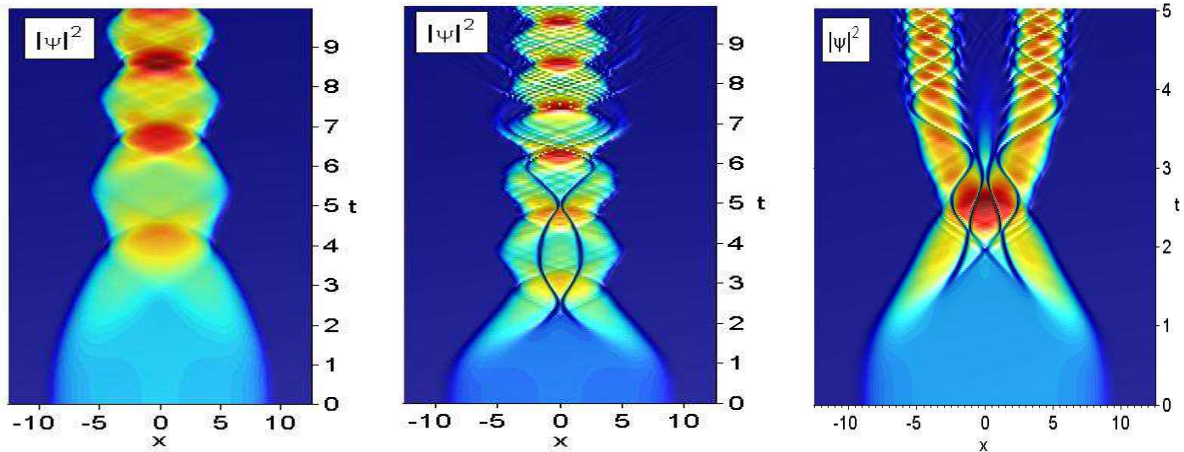


**Figure 4.** (Color online) Evolution of the wave function according to Eq. (1) with kernel (3), when the strength of the dipolar interaction is ramped up as  $d(t) = 2[1 + \tanh(\gamma t)]$ . Left panel: When the strength of the dipolar interaction is slowly raised with  $\gamma = 0.1$ , dark solitons do not emerge, while the TG gas performs contracting-expanding oscillations, preserving its integrity. Middle panel: At a moderately fast raise of  $d(t)$ , with  $\gamma = 0.3$ , a dark soliton-antisoliton pair is generated, making the quasi-particle bouncing of the dark solitons evident. Right panel: Swiftly ramping up  $d(t)$  with  $\gamma = 0.5$  gives rise to multiple generation of dark solitons and splitting of the original bright soliton. In time interval  $2 < t < 3$ , which precedes the breakup of the bright soliton, repeated dark-soliton collisions are observed. Oscillating dark solitons remain in the split parts of the original bright one.

background, the dark soliton is reflected back towards the center. This effect can be seen even after the original soliton splits, see the right panel in Fig. 4. Colliding at the center, two dark solitons interact repulsively and bounce back. This is a manifestation of the particle-like nature of dark matter-wave solitons, which was experimentally observed in BEC [38].

In order to highlight distinctive features of solitons in the dipolar TG gas, we have performed numerical simulations, similar to those shown in Fig. 4, also with the local counterpart of the original Eq. (1), i.e., Eq. (4), as shown in Fig. 5. In the case of local NLSE, the varying dipole moment  $d(t)$  is emulated by varying the coefficient of the cubic nonlinearity,  $\beta(t)$ , in Eq. (4). From comparing Figs. 4 and 5, one can observe drastically different behaviors. The most prominent distinction concerns the generation of long-lived oscillating dark solitons on top of the flat-top soliton in the nonlocal model. The other difference concerns the emission of linear waves under the varying coefficient of the cubic nonlinearity –  $d(t)$  or  $\beta(t)$ , respectively. Namely, the soliton of the local NLSE, Eq. (4), strongly radiates, while the soliton of nonlocal equation (1) shows almost no radiation. The mode of splitting of these two types of the solitons, when the coefficient in front of the cubic nonlinear local term is rapidly varied, is also very different (see middle and right panels in Figs. 4 and 5).

In experiments performed so far, dark solitons were created by optically imprinting a phase gradient onto a cigar shaped BEC [39]. The present approach, based on ramping



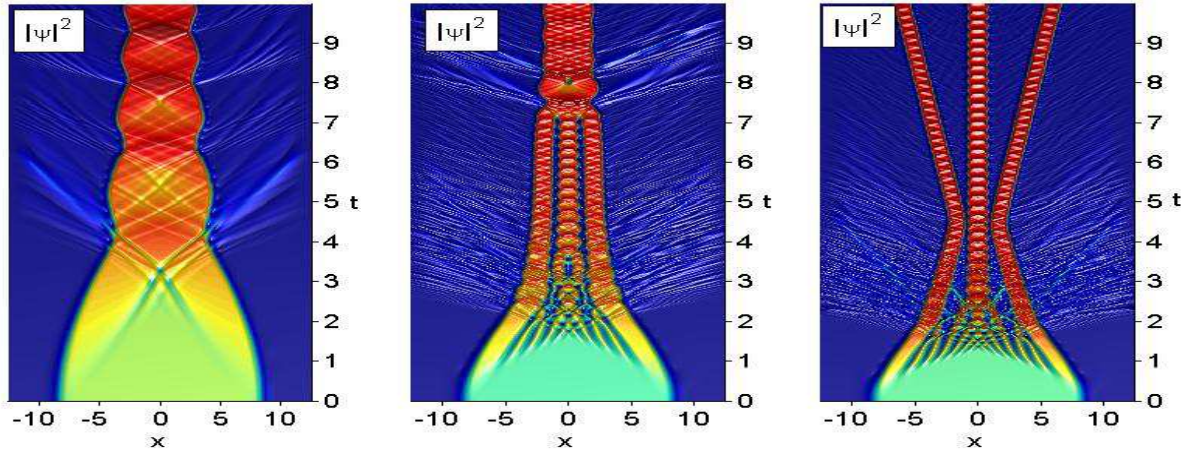


**Figure 5.** (Color online) Numerical simulations similar to those displayed in the previous figure, but for local equation (4). The coefficient in front of the cubic nonlinearity is varied in time according to  $\beta(t) = 4N[d(t)]^2$ , where  $d(t)$  is the same as in the previous figure. The initial state is the flat-top soliton of local cubic-quintic equation (4), which is shown in Fig. 3 by the solid red line. In contrast to the situation observed in the simulations of the nonlocal equation, dark solitons *do not* appear on top of the flat-top soliton.

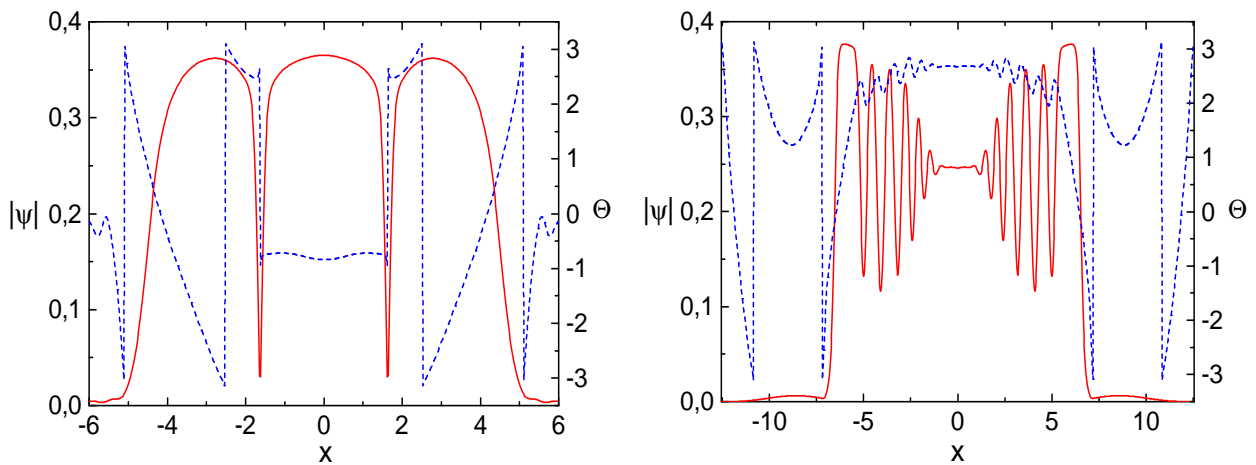


**Figure 6.** (Color online) Snapshots of the amplitude (red solid line, left axis) and phase (blue dashed line, right axis) of the wave function shown in Figs. 4 and 5, at  $t = 3.5$  (left panel) and  $t = 1.2$  (right panel), respectively. Left panel: A phase jump of  $\approx \pi$  across the density dips is the indication that the emerging excitations are dark solitons. Phase jumps outside the dips are usual  $2\pi$  phase wraps. Right panel: absence of phase jumps across density modulations implies that these are quasi-linear excitations, rather than dark solitons.

up the strength of the DD interactions, may be considered as an alternative approach to the controllable creation of dark solitons in quantum gases.

### 3.2. Free expansion of the TG gas

Expansion of a quantum gas released from the potential trap bears important information about correlations in the system. For instance, the momentum distribution of bosonic atoms, which expands after sudden removal of the trapping potential, has been the key evidence showing that the atoms exhibited a pronounced fermionic behavior, i.e., the TG regime has been achieved [1]. During the expansion of a 1D gas of hard-core bosons, the momentum-distribution function becomes equal to that of the equivalent non-interacting fermions. This phenomenon, known as the dynamical fermionization, is the most interesting manifestation of the Bose-Fermi duality [40]. Quantum correlations in the dynamically evolving TG gas in an OL were studied in Ref. [41].

Bright solitons in the TG gas with attractive DD interactions can offer additional possibilities in exploring properties of quantum gases. Specifically, since in the present setting the strong repulsion between bosonic atoms is balanced by the long-range DD attraction, the momentum distribution of a freely expanding gas, achieved by suddenly switching off or decreasing the strength of the DD interaction, develops from the initial spatial distribution specific to bright solitons (in contrast to that corresponding to the harmonic potential or box-shaped trap in previously studied settings). In the experiment, the DD interaction can be turned off by the rotation of the external magnetic field, or by eliminating the external dc electric field responsible for the induced electric dipole moment.

In Fig. 7 we illustrate the free expansion of the TG gas from the compacton-like soliton state shown in Fig. 1. Investigation of the scaling law governing the expansion of the TG gas of dipolar atoms, as well as of its momentum distribution, may be interesting topics for subsequent studies.

## 4. Interactions and collisions of dipole solitons

The wave-particle duality of solitons can be most clearly observed in their interactions and collisions. While “genuine” solitons in integrable models collide strictly elastically, solitons of non-integrable models show complex collision behaviors, ranging from almost elastic to fully destructive. Inelasticity of collisions show up as significant emission of linear waves resulting from the collision, merger of colliding solitons into a single dynamically evolving wave packet (including a possible transition to the wave collapse), splitting of solitons, and multiple generation of secondary solitons.

Collisions of matter-wave solitons composed of cold atoms with contact interactions have been extensively studied, both in numerical simulations [42] and in real experiments [43]. In particular, inelasticity in collisions of solitons described by the local NLSE with self-focusing cubic and quintic terms, the latter one generated by the deviation of the

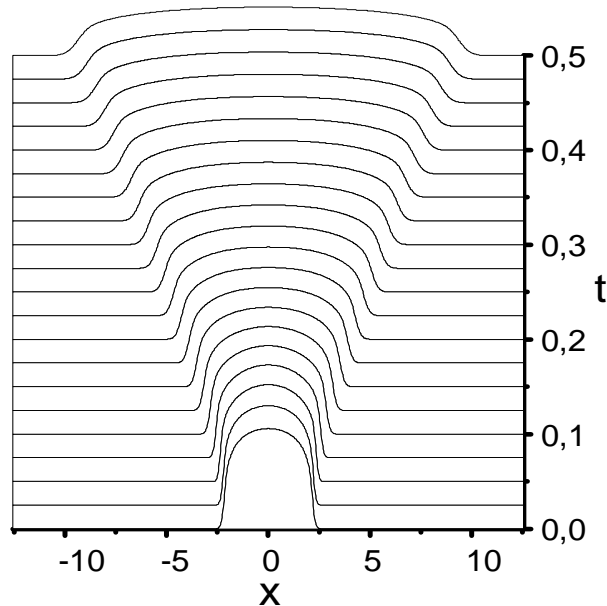


**Figure 7.** The free expansion of the TG gas after the strength of the dipolar interaction was suddenly dropped to zero. The initial state is the compacton-like soliton depicted in Fig. 1 by the dashed line.

effective equation from the one-dimensionality, were analyzed in Ref. [44].

Collision of matter-wave solitons in BEC with competing cubic local and dipolar interactions has recently been studied by means of numerical simulations in Ref. [21]. Here, we explore collisions between dipole solitons in the TG-gas model. Since the objective is to reveal features introduced by the long-range dipolar forces, we focus on the interactions and collisions between compacton-like solitons, whose properties are dominated by dipolar forces.

There are essential differences of the present model in comparison to work [21]: the self-defocusing nonlinear term is here quintic, and the arrangement of interacting solitons is different. Namely, in our case one soliton (the “target”) is at rest at the origin ( $x = 0$ ), while the other (the “missile”) is set in motion towards the target. This setting allows us to explicitly investigate the momentum exchange between the colliding solitons.

An important conclusion suggested by the numerical experiments is that the long-range attraction is the dominant force between the interacting solitons. This nonlocal force is phase-independent and much stronger than usual short-range interaction forces which depend on the phase shift between the solitons.

In the first set of the numerical experiments, we set two quiescent (zero-velocity) dipole solitons at distance  $\delta x = 4\pi$  from each other, and observed their evolution. In either case of in-phase (see Fig. 8 (a)) and  $\pi$  - out-of-phase (not shown) pairs of the solitons, they attracted each other and merged into a breather. The fact that the merger time in both cases was almost the same ( $t \simeq 6$ ) indicates that the phase-dependent short-range interaction force has played no tangible role in the dynamics.

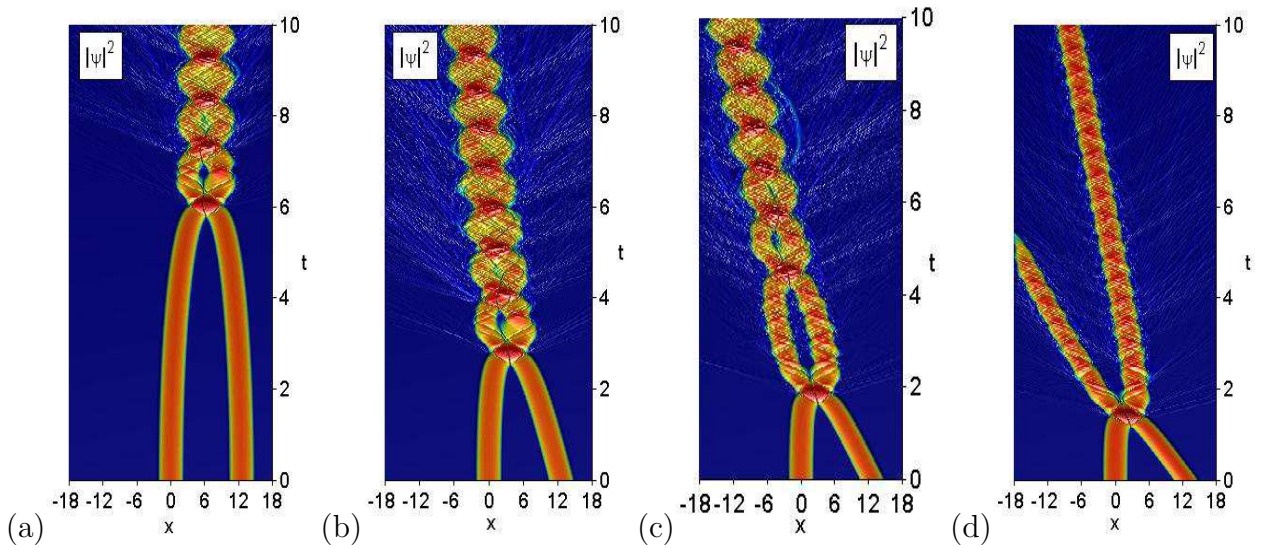


**Figure 8.** (Color online) Collisions of two compacton-like solitons (shown in Fig. 1 by the dashed line) placed at distance  $\delta x = 4\pi$ . (a) Two quiescent (zero-velocity) dipole solitons attract each other and merge into a breather, whose center-of-mass is still. (b)-(d) When the right soliton is set in motion with velocity  $v_0$  towards the left (quiescent) one, the outcome of the collision depends on the initial velocity. At moderate velocities,  $v_0 = -2$  (b) and  $v_0 = -4$  (c), solitons merge into a breather, moving in the same direction as the “missile” soliton. At larger velocity  $v_0 = -6$  (d), the two solitons separate after the collision. The “target” acquires the velocity, while the “missile” reduces its velocity, in accordance with the conservation of the total momentum.

Next, we consider collisions between moving solitons. With this objective in mind, we prepared the initial state with one soliton set at the origin ( $x = 0$ ) with zero velocity ( $v = 0$ ), and the other one placed at  $x = 4\pi$  with finite velocity  $v_0$ . General features of soliton collisions can be summarized as follows (see Fig. 8 (b), (c), (d)): at moderately small velocities, e.g.,  $v_0 = -2$ , solitons merge into a single breather. In fact, the dipolar attraction between the solitons facilitates the merger. At greater velocities (such as  $v_0 = -4$ ), the initially moving soliton passes through the quiescent one, imparting to it a small velocity in the same direction. In this case, although the solitons separate after the collision, the dipolar attraction between them overcomes the trend to the separation and solitons again merge into a single breather. At still greater velocities (e.g.,  $v_0 = -6$ ), the two solitons separate and fly apart overcoming the dipolar attraction. The conservation of the total momentum of the colliding solitons can be clearly observed in these numerical experiments.

## 5. Conclusions

In this work, our aim was to study the existence, stability and basic dynamical properties of bright one-dimensional solitons based on the balance between the local (hard-core) repulsion and long-range DD (dipole-dipole) attraction between atoms in the model of

the TG gas. It was found that, depending on the number of atoms and strength of the DD interaction, the solitons assume flat-top or compacton-like shapes. For solitons of the former type, solution of the local cubic-quintic NLSE with competing nonlinearities is found to be a good approximation. Numerical simulations of the underlying nonlocal equation with a variable strength of the DD interaction have revealed various dynamical regimes, including the formation of dark solitons on top of a bright one (of the flat-top type), particle-like collisions between them, splitting of the flat-top solitons, and self-similar ballistic expansion of the gas after dropping the DD attraction. Collisions between bright solitons of the compacton type have been investigated in different regimes. The strong dipolar attraction between the solitons explains that, in many cases, the colliding solitons merge into a breather.

## Acknowledgements

We thank E N Tsoy for valuable discussions and helpful suggestions. F Kh A and B B B acknowledge partial support from the Fund for Fundamental Research of the Uzbek Academy of Sciences under Grant No. 10-08. M S acknowledges partial support from the Istituto Nazionale di Fisica Nucleare (INFN), Gruppo Collegato di Salerno, Sezione di Napoli. The work of B A M was supported, in a part, by the German-Israel Foundation through grant No. 149/2006.

## References

- [1] Paredes B, Widera A, Murg V, Mandel O, Folling S, Cirac I, Shlyapnikov G V, Hansch T W and Bloch I 2004 *Nature* **429** 277  
Kinoshita T, Wenger T and Weiss D S 2004 *Science* **305** 1125
- [2] Tonks L 1936 *Phys. Rev.* **50**, 955  
Girardeau M 1960 *J. Math. Phys.* **1** 516  
Lieb E H and Liniger W 1963 *Phys. Rev.* **130** 1605  
Lieb E H 1963 *Phys. Rev.* **130** 1616
- [3] Yukalov V I and Girardeau M D 2005 *Laser Phys. Lett.* **2** 375
- [4] Kolomeisky E B, Newman T J, Straley J P and Qi X 2000 *Phys. Rev. Lett.* **85** 1146
- [5] Damski B 2004 *J. Phys. B: At. Mol. Phys.* **37** L85
- [6] Bhaduri R K, Ghosh S, Murthy M V N and Sen D 2001 *J. Phys. A: Math. Gen.* **34** 6553
- [7] Frantzeskakis D J, Proukakis N P and Kevrekidis P G 2004 *Phys. Rev. A* **70** 015601
- [8] Abdullaev F Kh and Salerno M 2005 *Phys. Rev. A* **72** 033617
- [9] Adhikari S K and Malomed B A 2007 *Europhys. Lett.* **79**, 50003  
Adhikari S K and Malomed B A 2009 *Physica D* in press
- [10] Alfimov G L, Konotop V V and Pacciani P 2007 *Phys. Rev. A* **75** 023624
- [11] Minguzzi A, Vignolo P, Chiofalo M L and Tosi M P 2001 *Phys. Rev. A* **64** 033605
- [12] Abdullaev F Kh and Garnier J 2004 *Phys. Rev. A* **70** 053604
- [13] Griesmaier A, Werner J, Hensler S, Stuhler J and Pfau T 2005 *Phys. Rev. Lett.* **94** 160401  
Stuhler J, Griesmaier A, Koch T, Fattori M, Pfau T, Giovanazzi S, Pedri P and Santos L 2005 *Phys. Rev. Lett.* **95** 150406  
Griesmaier A, Stuhler J, Koch T, Fattori M, Pfau T and Giovanazzi S 2006 *Phys. Rev. Lett.* **97** 250402

- Lahaye T, Koch T, Fröhlich B, Fattori M, Metz J, Griesmaier A, Giovanazzi S and Pfau T 2007 *Nature* **448** 672
- Koch T, Lahaye T, Metz J, Fröhlich B, Griesmaier A and Pfau T 2008 *Nature Phys.* **4** 218
- [14] Lahaye T, Metz J, Fröhlich B, Koch T, Meister M, Griesmaier A, Pfau T, Saito H, Kawaguchi Y and Ueda M 2008 *Phys. Rev. Lett.* **101** 080401
- [15] Griesmaier A 2007 *J. Phys. B: At. Mol. Phys.* **40** R91
- [16] Deiglmayr J, Grochola A, Repp M, Mörtlbauer K, Glück C, Lange J, Dulieu O, Wester R and Weidemüller M 2008 *Phys. Rev. Lett.* **101** 133004
- [17] Marinescu M and You L 1998 *Phys. Rev. Lett.* **81** 4596
- Giovanazzi S, O'Dell D H J and Kurizki G 2002 *Phys. Rev. Lett.* **88** 130402
- Mazets I E, O'Dell D H J, Kurizki G, Davidson N and Schleich W P 2004 *J. Phys. B: At. Mol. Phys.* **37** S155
- Low R, Gati R, Stuhler J and Pfau T 2005 *Europhys. Lett.* **71** 214
- [18] Pedri P and Santos L 2005 *Phys. Rev. Lett.* **95** 200404
- Lashkin V M 2007 *Phys. Rev. A* **75** 043607
- Tikhonenkov I, Malomed B A and Vardi A 2008 *Phys. Rev. A* **78** 043614
- [19] Tikhonenkov I, Malomed B A and Vardi A 2008 *Phys. Rev. Lett.* **100** 090501
- [20] Malomed B A, Mihalache D, Wise F and Torner L 2005 *J. Opt. B: Quantum Semiclass. Opt.* **7** R53
- [21] Cuevas J, Malomed B A, Kevrekidis P G and Frantzeskakis D J 2009 *Phys. Rev. A* **79**, 053608
- Gligorić G, Maluckov A, Hadžievski L and Malomed B A 2009 *J. Phys. B: At. Mol. Phys.* in press
- [22] Gligorić G, Maluckov A, Hadžievski L and Malomed B A 2008 *Phys. Rev. A* **78** 063615
- Gligorić G, Maluckov A, Hadžievski L and Malomed B A 2009 *Phys. Rev. A* **79** 053609
- [23] Skupin S, Bang O, Edmundson D and Królikowski W 2006 *Phys. Rev. E* **73** 066603
- Rotschild C, Cohen O, Manela O, Segev M and Carmon T 2005 *Phys. Rev. Lett.* **95** 213904
- [24] Mihalache D, Mazilu D, Lederer F, Crasovan L C, Kartashov Y V, Torner L and Malomed B A 2006 *Phys. Rev. E* **74** 066614
- Kartashov Y V, Vysloukh V A and Torner L 2009 *Phys. Rev. A* **79** 013803
- [25] Pushkarov Kh I, Pushkarov D I and Tomov I V 1979 *Opt. Quant. Electr.* **11** 471
- [26] Nakamura A 1977 *J. Phys. Soc. Jpn.* **42** 1824
- Wang X, Brown D W, Lindenberg K and West B J 1988 *Phys. Rev. A* **37** 3557
- Parola A, Salasnich L and Reatto L 1998 *Phys. Rev. A* **57** R3180
- Mitchell D J and Snyder A W 1999 *J. Opt. Soc. Am. B* **16** 236
- Królikowski W, Bang O, Rasmussen J J and Wyller J 2001 *Phys. Rev. E* **64** 016612
- Cohen O, Buljan H, Schwartz T, Fleischer J W and Segev M 2006 *Phys. Rev. E* **73** 015601(R)
- [27] Snyder A W and Mitchell D J 1997 *Science* **276** 1538
- [28] Conti C, Peccianti M and Assanto G 2004 *Phys. Rev. Lett.* **92** 113902
- [29] Królikowski W and Bang O 2001 *Phys. Rev. E* **63** 016610
- [30] Sinha S and Santos L 2007 *Phys. Rev. Lett.* **99** 140406
- [31] Vakhitov M G and Kolokolov A A 1973 *Radiophys. Quantum Electron.* **16** 783
- [32] Reinhardt W P and Clark C W 1997 *J. Phys. B: At. Mol. Phys.* **30** L785
- Busch Th and Anglin J R 2000 *Phys. Rev. Lett.* **84** 2298
- [33] Press W H, Teukolsky S A, Vetterling W T and Flannery B P 1996 *Numerical Recipes. The Art of Scientific Computing* (Cambridge: Cambridge University Press)
- [34] Agrawal G P 1995 *Nonlinear Fiber Optics*, 2nd ed. (Academic Press: New York)
- [35] Chiofalo M L, Succi S and Tosi P 2000 *Phys. Rev. E* **62** 7438
- [36] Abramowitz M and Stegun I A 1964 *Handbook of Mathematical Functions*, (National Bureau of Standards, Washington)
- [37] Goral K, Brewczyk M and Rzazewski K 2003 *Phys. Rev. A* **67** 025601
- [38] Becker C, Stellmer S, Soltan-Panahi P, Dorscher S, Baumert M, Richter E M, Kronjäger J, Bongs K and Sengstock K 2008 *Nature Phys.* **4** 496

- [39] Carr L D, Brand J, Burger S and Sanpera A 2001 *Phys. Rev. A* **63** 051601  
Burger S, Carr L D, Ohberg P, Sengstock K and Sanpera A 2002 *Phys. Rev. A* **65** 043611  
Weller A, Ronzheimer J P, Gross C, Esteve J, Oberthaler M K, Frantzeskakis D J, Theocharis G and Kevrekidis P G 2008 *Phys. Rev. Lett.* **101** 130401
- [40] Rigol M and Muramatsu A 2005 *Phys. Rev. Lett.* **94** 240403  
Minguzzi A and Gangardt D M 2005 *Phys. Rev. Lett.* **94** 240404
- [41] Pezer R and Buljan H 2007 *Phys. Rev. Lett.* **98** 240403
- [42] Parker N G, Martin A M, Cornish S L and Adams C S 2008 *J. Phys. B: At. Mol. Phys.* **41** 045303  
Martin A D, Adams C S and Gardiner S A 2008 *Phys. Rev. A* **77** 013620
- [43] Martin A D, Adams C S and Gardiner S A 2007 *Phys. Rev. Lett.* **98** 020402
- [44] Khaykovich L and Malomed B A 2006 *Phys. Rev. A* **74** 023607